Wigner Crystallization in $Na_3Cu_2O_4$ and $Na_8Cu_5O_{10}$ Chain Compounds

P. Horsch, M. Sofin, M. Mayr, and M. Jansen

Max-Planck-Institut für Festkörperforschung, Heisenbergstrasse 1, D-70569 Stuttgart, Germany

(Received 15 September 2004; published 23 February 2005)

We report the synthesis of novel edge-sharing chain systems $Na_3Cu_2O_4$ and $Na_8Cu_5O_{10}$, which form insulating states with commensurate charge order. We identify these systems as one-dimensional Wigner lattices, where the charge order is determined by long-range Coulomb interaction and the number of holes in the d shell of Cu. Our interpretation is supported by x-ray structure data as well as by an analysis of magnetic susceptibility and specific heat data. Remarkably, due to large second neighbor Cu-Cu hopping, these systems allow for a distinction between the (classical) Wigner lattice and the $4k_F$ charge-density wave of quantum mechanical origin.

DOI: 10.1103/PhysRevLett.94.076403 PACS numbers: 71.10.Fd, 71.28.+d, 74.72.Jt, 75.10.Pq

The role of strong electron correlations and the concomitant appearance of *spatially modulated charge structures* constitutes a central issue in current solid state physics [1]. The most prominent examples are charge stripes in high-T_c superconductors, which have been discovered first as static modulations in the CuO_2 planes of $La_{1.6-x}Nd_{0.4}Sr_xCuO_4$ [2]. The high-T_c enigma has at the same time stimulated the flourishing field of low-dimensional cuprates composed of Cu-O chains and ladders [3] with the hope of gaining new insights overlooked so far in the layered cuprates. One important aspect is the role of long-range Coulomb interaction in strongly correlated systems, which gives rise to metal/insulator stripe structures in organic charge-transfer compounds[4].

Following a recently discovered new route in the synthesis of alkalioxometallates [5], we were able to synthesize several members of a new class of quasi-1D cuprates $Na_{1+x}CuO_2$. These *intrinsically doped* edge-sharing chain systems provide a unique opportunity to study the condensation of charge order (CO) at high temperature and the formation of spatially modulated Heisenberg spin systems at low temperature. Edge-sharing chains are also building blocks of the intensively studied $Sr_{14-x}Ca_xCu_{24}O_{41}$ system; due to exchange of electrons with ladders, however, the degree of doping is difficult to determine [6]. Here, we argue that these doped chains can be understood as realizations of one-dimensional Wigner lattices (WL) [7], as introduced by Hubbard [8] in the late 1970s in connection with TCNQ charge-transfer salts. He suggested that the distribution of electrons is controlled by the Coulomb interaction rather than by the kinetic energy ($\sim$bandwidth), such that they form a *generalized Wigner lattice* on the underlying TCNQ chain structure. This view suggests a strikingly different nature of charge excitations, namely, as domain walls with fractional charge rather than particle-hole excitations as in common metals and semiconductors. Hubbard's proposal, however, can be challenged on the grounds that the resulting periodicity of charge modulation can alternatively be explained by a $4k_F$ charge-density wave (CDW) [9–11] arising from short-range interactions alone and an instability of the Fermi surface, where k_F denotes the Fermi momentum.

The edge-sharing arrangement of CuO_4 squares meets the WL criterion of small band width in an optimal way due to the almost 90 ° Cu-O-Cu bonds (Fig. 1). Unexpected complexity is added because, apart from a small nearest-neighbor hopping matrix element t_1, there is also a second neighbor hopping t_2, which is larger as a consequence of the structure. While this unusual feature does not affect the classical WL order imposed by the Coulomb interaction, it changes the Fermi surface topology, and thereby allows to distinguish the WL from the CDW on the basis of the modulation period.

These systems provide a first example where an unambiguous distinction between the generalized WL and a Fermi surface related $4k_F$ CDW is possible. We also show that for these edge-sharing compounds even the magnetic and thermodynamic properties can only be explained by invoking a WL ground state emerging from the truly long-ranged Coulomb interaction.

Samples were prepared by the azide/nitrate route [5]. As a source for the alkali metal component, mixtures of the respective alkali azides and nitrates (or nitrites) are used instead of the alkali oxides. Conveniently, besides the metals' ratio, also the oxygen content and thus the degree and kind of doping of the desired product can be effectively controlled using the weighed portions of the starting materials. Following this procedure the title compounds $Na_3Cu_2O_4$ ($x = 1/2$) and $Na_8Cu_5O_{10}$ ($x = 3/5$) have been prepared as microcrystalline, pure phases in gram amounts. The new oxocuprates (II/III) belong to the compositional series $Na_{1+x}CuO_2$, with the end members $NaCuO_2$ [12] and the still elusive Na_2CuO_2. The most prominent structural feature, common to all representatives known thus far, is a one-dimensional polyanion CuO_2^{n-} constituted of CuO_4 square units sharing edges in transposition. These anionic entities are embedded by sodium ions which achieve coordination numbers of 4–6 with Na-O bond lengths ranging from 2.27 to 2.79 Å. The geometric data as determined by single crystal structural analyses

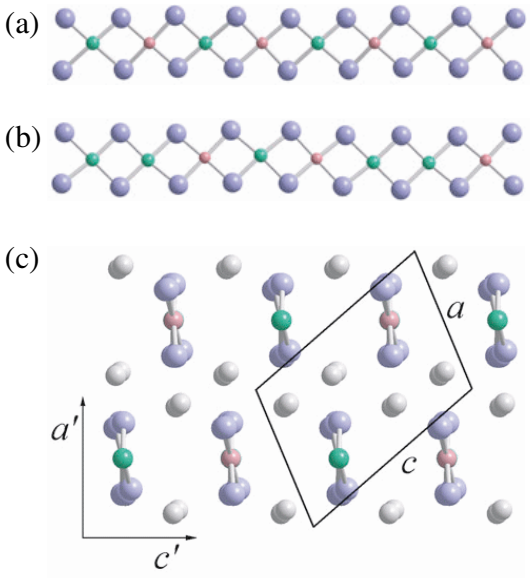

FIG. 1 (color). Structure of edge-sharing copper-oxygen chains along the b direction in $Na_3Cu_2O_4$ (a) and $Na_8Cu_5O_{10}$ (b), where Cu^{2+} and Cu^{3+} are marked by green and red circles, and O^{2-} (Na^+) by large blue (gray) circles, respectively. (c) View on the a-c plane of $Na_3Cu_2O_4$. For convenience we introduce a Cartesian system a', $b'||b$, c' in addition to crystallographic coordinates.

give clear evidence for a CO at the Cu sites (Fig. 1). The Cu^{3+} and Cu^{2+} oxidation states can be clearly identified by the Cu-O distances, which for $Na_3Cu_2O_4$ are in the range 1.826–1.857 and 1.923–1.943 Å, respectively. The way of linking the primary structural units together with the variations of the copper to oxygen distances inevitably leads to deviations of the O-Cu-O angles from the ideal 90°. As monitored by differential scanning calorimetry measurements CO disappears above the WL melting temperature $T_m = 455$ and 540 K for $Na_3Cu_2O_4$ and $Na_8Cu_5O_{10}$, respectively. The dc and ac conductivity measurements show also a clear transition from an Arrhenius behavior below T_m to an almost temperature independent conductivity regime above T_m.

For a theoretical analysis one has to recognize that Cu^{2+} is in a d^9 configuration with spin 1/2, while Cu^{3+} is in a d^9-ligand hole (d^9L_h) singlet state, also known as Zhang-Rice singlet [13]. In contrast to high-T_c cuprates, the edge-sharing geometry [Fig. 1(a) and 1(b)] leads to strongly reduced hopping matrix elements. This sets the stage for the long-range Coulomb force as dominant interaction

$$H_{\mathrm{Coul}} = U\sum_i n_{i,\uparrow}n_{i,\downarrow} + \sum_{i,l\geq 1} V_l n_i n_{i+l}, \qquad (1)$$

where the on-site interaction U suppresses charge fluctuations involving Cu^{1+} (d^{10}) configurations. Here we associate the d^9L_h (d^9,d^{10}) ionization state with 0 (1, 2) electrons, respectively, and $n_{i,\sigma}$ ($\sigma = \uparrow, \downarrow$) counts the number of electrons with spin σ, while $n_i = n_{i,\uparrow} + n_{i,\downarrow}$. The Coulomb interaction V_l in general is screened by the polarization of neighboring chains as well as by core electrons [8]. Here we assume a generic Coulomb law $V_l = \frac{V}{l}$, $l = 1, 2, \ldots$ [14]. Crucial for the following is that the interaction is long ranged and convex, i.e., $V_l'' = V_{l-1} - 2V_l + V_{l+1} > 0$.

For commensurate doping concentration $x = m/n$ the interaction V_l selects a particular CO pattern [8]. This pattern is immediately obvious for filling fractions $x = 1/2$ and 3/4 [Fig. 2(a) and 2(d)] which involve an equidistant arrangement of the Cu^{3+} sites (circles in Fig. 2). For a general ratio $x = m/n$ this leads to complex structures with unit cell size n (in units of the Cu-Cu distance $b' = 1$). In the case of $x = 3/5$, we encounter in Fig. 2(b) the charge order observed for $Na_8Cu_5O_{10}$. Charge localization, however, is not perfect in Wigner insulators as electrons still undergo virtual transitions to neighboring sites [Fig. 2(a*) and 2(b*)] in order to retain partially their *kinetic energy*. The energy of the lowest excitations and the impact of kinetic energy depend strongly on x; e.g., the energy of the excitation in Fig. 2(a*) relative to the ground state Fig. 2(a) is $\sim V_2''$ while the excitation for $x = 3/5$ in Fig. 2(a*) is $\sim V_5''$, about an order of magnitude smaller. To investigate the role of kinetic energy we explore the dynamics of electrons starting from the 1D *Hubbard-Wigner model* $H_{\mathrm{HW}} = H_{\mathrm{Coul}} + H_{\mathrm{Kin}}$ [8], where

$$H_{\mathrm{Kin}} = -\sum_{i,l,\sigma} t_l (c^+_{i+l,\sigma}c_{i,\sigma} + c^+_{i,\sigma}c_{i+l,\sigma}) \qquad (2)$$

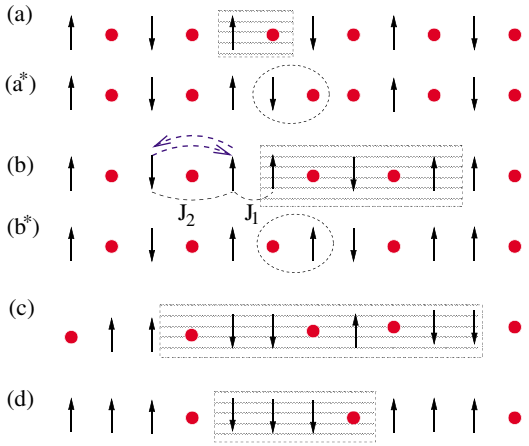

FIG. 2 (color online). Wigner charge order resulting from Coulomb repulsion and associated modulated Heisenberg spin structure for $x = 1/2, 3/5, 5/8$, and 3/4 doping (a)–(d). The spin-1/2 of Cu^{2+} (arrows) is responsible for magnetism; Cu^{3+} (circles) is nonmagnetic. The spin arrangement is that expected for ferromagnetic exchange J_1 and antiferromagnetic J_2, where the two excitations $d^9d^9 \leftrightarrow d^9L_hd^{10}$ contributing to J_2 are indicated by dashed arrows in (b). The charge unit cells (shaded) contain 2, 5, 8, 4 sites, respectively. The structures (a) and (b) are realized in $Na_3Cu_2O_4$ and $Na_8Cu_5O_{10}$, respectively, and the dashed circles in (a*) and (b*) indicate charge excitations $\propto V$ in these structures. (d) Typical modulation for charge stripes in high-T_c cuprates [2].

describes the hopping of an electron with spin σ. Because of the almost 90° Cu-O-Cu angle, the hopping t_1 between nearest-neighbor Cu sites results mainly from direct d-d exchange, while t_2 originates from hopping via a Cu-O-O-Cu path [15] (Fig. 1), leading to the remarkable fact $|t_2| > |t_1|$. We adopt here as typical values $t_1 \sim 63$ meV, $t_2 \sim 94$ meV, derived from *ab initio* band structure calculations for the Cu^{2+} edge-sharing reference system Li_2CuO_2 [16]. These values are indeed much smaller than our estimates for $U \sim 3.8$ eV and $V \sim 1.5$ eV based on optical data for Li_2CuO_2 [15].

Using exact diagonalization we have calculated the static structure factor $S_c(q)$ for chains up to 25 sites. The peaks of $S_c(q)$ at $q_w = 1.2\pi$ (and at $0.8\pi = 2\pi - q_w$) are characteristic for a WL modulation at $x = 3/5$ [Fig. 3(a)]. Since the magnetic energy scale is much smaller than the Coulomb interaction V, the charge structure can be determined by disregarding spin degrees of freedom, namely, in terms of spinless fermions (SF). The SF-CDW arises as an instability due to low-energy scattering between the two Fermi points at $\pm k_{\mathrm{SF}}$ which lead to a singularity in the charge susceptibility $\chi_c^0(q)$ at $q = 2k_{\mathrm{SF}} (= 4k_F)$. Subsequent inclusion of interactions is expected to change the character of a singularity, yet not the momentum at which the singularity occurs. This explains the origin of the $4k_F$ CDW instability in interacting 1D systems and, as $4k_F = 2\pi m/n$, the coincidence with the modulation period n of the WL.

The equivalence of WL and CDW periodicity disappears when $t_2 > \alpha t_1$ ($\alpha = 0.38$ at $x = 0.6$); then there are four instead of two Fermi points leading to new singularities in

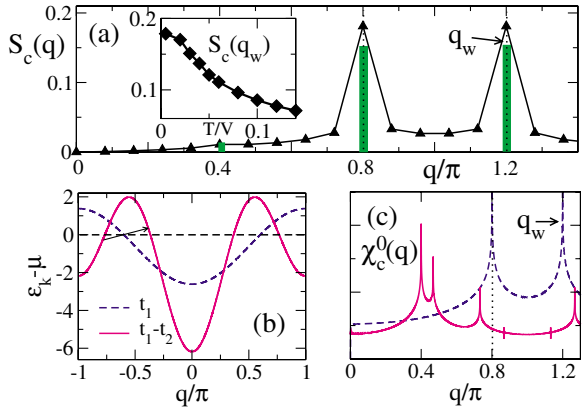

FIG. 3 (color online). (a) Static charge structure factor $S_c(q)$ calculated for interacting spinless fermions and $t_1 = 0.04$ V, $t_2 = 0.06$ V at $x = 0.6$ indicates the instability towards WL ordering with modulation $q_w = 1.2\,\pi$ (solid line as guide to the eye). Inset shows the temperature dependence of $S_c(q_w)$. (b) Comparison of electron dispersions for a system with nearest-neighbor hopping $t_1 (= 1)$ only (dashed line) and for $t_1 = 1$, $t_2 = 1.5$ (solid line) with the Fermi energy indicated by a horizontal line. (c) While the charge susceptibility $\chi_c^0(q)$ for noninteracting spinless fermions in the t_1 model shows a logarithmic divergence at $2k_{\mathrm{SF}} = q_w$, the singularities of the t_1-t_2 model are at different momenta.

$\chi_c^0(q)$ [Fig. 3(b) and 3(c)] and to a shift of the original singularity away from $4k_F = q_w$. In this case the standard tools of many-body theory such as bosonization [11] suggest a change of the modulation period. This, however, is not reflected in the experiment and is also not observed in our numerical results for $S_c(q)$ [Fig. 3(a)]. In fact, the singularity remains at q_w up to a value $t_2 \sim 4t_1$, a striking manifestation that the structure is robust and controlled by the long-range Coulomb interaction [17]. The calculated $S_c(q)$ shows besides the main peak at q_w a weak higher harmonic feature at $q = 2q_w - 2\pi$, consistent with the relative intensities of structural reflexes calculated from the experimentally determined Cu ion positions [vertical bars in Fig. 3(a)]. Further results [inset Fig. 3(a)] reveal that WL correlations persist up to temperatures $k_B T \sim 0.05$ V, consistent with experiment.

The magnetic susceptibility $\chi(T)$ was measured in the temperature range from 5 to 350 K using a SQUID magnetometer. The data [Fig. 4(a)] reveal strikingly different temperature dependences for the two compounds: $\chi(T)$ for $Na_3Cu_2O_4$ displays some similarity with a nearest-neighbor Heisenberg antiferromagnetic chain [18], whereas the $Na_8Cu_5O_{10}$ data show continuous increase down to low temperature until its maximum near 25 K is reached. Both systems reveal antiferromagnetic correlations, yet magnetic order is observed only for $Na_8Cu_5O_{10}$ at $T_N = 23.5$ K. For a calculation of $\chi(T)$ we assume that the spins remain fixed at their positions $\mathbf{R}_i$ as given by the structural analysis and by H_{HW} (Fig. 2). This leads to a generalized Heisenberg model

$$H_{\mathrm{Heis}} = \frac{1}{2}\sum_{i,j} J(\mathbf{R}_i - \mathbf{R}_j)\mathbf{S}_i \cdot \mathbf{S}_j, \qquad (3)$$

where the exchange constants depend on the distance $|\mathbf{R}_i - \mathbf{R}_j|$ between the spins and on the direction (parallel to the chains or perpendicular). For $x = 0.5$, only the exchange constants $J_2, J_4, \ldots$ along the chains contribute, while for $x = 0.6$, $J_1, J_2, J_3, \ldots$ are relevant. Apart from the modulated spin pattern, superexchange [19] in WL's shows further novel features, namely, fluctuations (a) of spin positions and (b) of antiferromagnetic exchange integrals $J_l \sim 4t_l^2/[U + \Delta(V)]$ due to the low-energy charge fluctuations. The energy shifts $\Delta(V)$ due to V_l depend on the WL structure and are in general different for left (right) scattering processes [see Fig. 2(b)]. The exchange constants may be estimated from the parameters specified above. The largest coupling is $J_2 \approx 100$–200 K resulting from superexchange via a Cu-O-O-Cu path. Because of the almost 90° Cu-O-Cu bond angle J_1 exchange is smaller [15]. Yet in the case of J_1 there are additional exchange contributions that have to be taken into account. The most important of these involve O p^4 configurations with Hund interaction on oxygen [20], such that the total J_1 may become negative.

We have used finite temperature diagonalization (FTD) [21] to calculate $\chi(T)$ for $Na_3Cu_2O_4$ studying chains up to

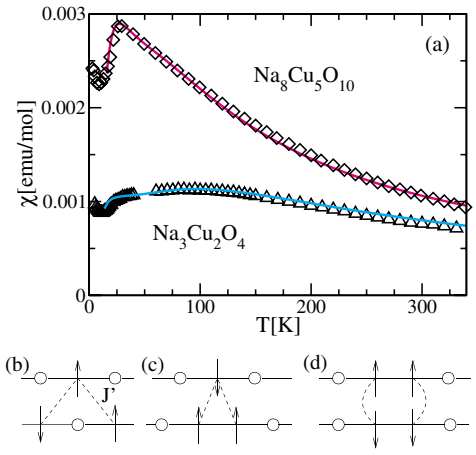

FIG. 4 (color online). (a) Temperature dependence of susceptibility $\chi(T)$ for $Na_3Cu_2O_4$ and $\chi/3$ for $Na_8Cu_5O_{10}$. Multiplication by $1/3$ in the latter case provides a comparison per spin. Theoretical results calculated by FTD are indicated by lines (exchange constants are given in the text). Sketch of interchain interactions used in the calculation of $\chi(T)$: for $Na_3Cu_2O_4$ (b) the magnetic exchange J' is frustrated due to triangular coordination, while it is not frustrated for $Na_8Cu_5O_{10}$ both along the a' direction (c) and the c' direction (d).

$N = 48$ sites (24 spins). Good agreement with experiment was achieved with $J_2 = 172$, $J_4 = 17$ K, and 1.97 for the g factor. The small antiferromagnetic interchain coupling $J' = 34$ K [Fig. 4(b)] is frustrating as the correlations on b' chains are antiferromagnetic. The interaction J' has been taken into account in a mean-field approach [18] $\chi(T) = \chi_s(T)/[1 + z'|J'|\chi_s(T)]$, where $\chi_s(T)$ is the result for a single chain, while z' counts the number of spins on neighboring chains ($z' = 4$). The frustrated geometry implies a spin gap Δ_s [22]. For the present parameter set we obtain $\Delta_s \sim 4$ K, consistent with our analysis of the specific heat data. A thorough analysis of the Curie contribution, using specific heat and susceptibility data independently, reveals that there are about $\sim 1\%$ impurities per Cu ion present in both $Na_3Cu_2O_4$ and $Na_8Cu_5O_{10}$ [23].

In the case of $Na_8Cu_5O_{10}$ the correlations along the b chains turn out to be of *ferrimagnetic* nature. A full FTD calculation of a double chain was necessary to account for the AF interchain exchange J' along the c' direction [Fig. 4(d)], while the coupling of chains along the a' direction [Fig. 4(c)] was treated within mean field. This implies ferrimagnetic a'-b' planes, which are antiferromagnetically coupled along the c' direction. A satisfactory description was found for $J_1 = -22$ K, $J_2 = 113$ K, $J' = 21$ K, and $g = 2.0$. The ferromagnetic interaction J_1 is the origin of the strong enhancement of $\chi(T)$ in the $x = 0.6$ system. The reduced value of J_2 can be explained by low-energy charge fluctuations [Fig. 2(b*)], which involve a fluctuation of spin positions, i.e., $J_2^{\text{eff}} \simeq (1 - p)J_2 + pJ_1$ and a larger probability p than for $x = 1/2$.

The strong variation of $\chi(T)$ in $Na_8Cu_5O_{10}$ should be interpreted as a crossover between two regimes. While at high temperature, $\chi(T)$ is controlled by the individual spins, at low temperatures only *effective* spins $1/2$, formed by three spins which are coupled by the largest interaction J_2, are relevant [Fig. 2(b)]. The composite nature of the effective spins and their internal energy level structure becomes relevant in the intermediate temperature region. The interaction between these effective spins is renormalized to $J_1^{\text{eff}} = \frac{4}{9}[J_1 - J_3 + \frac{1}{4}J_5]$. Thus, the peculiar low-T behavior of $\chi(T)$ is controlled by an interplay of the small J_1^{eff} between effective spins, resulting from WL order, and the interchain interactions.

Finally, the new compounds provide a unique opportunity to study the competition between two entirely different states: the classical WL dictated by the long-range Coulomb interaction and the CDW of quantum mechanical origin, i.e., resulting from a Fermi surface instability. These materials highlight the importance of long-range Coulomb interaction in strongly correlated systems and provide a one-dimensional test ground for the study of charge stripe formation.

We thank E. Brücher and G. Siegle for the susceptibility and specific heat measurements, and L. Capogna, B. Keimer, W. Metzner, and A. M. Oleś for discussions.

[1] J. Orenstein and A. J. Millis, Science **288**, 468 (2000).
[2] J. M. Tranquada *et al.*, Nature (London) **375**, 561 (1995); *ibid.***429**, 534 (2004).
[3] E. Dagotto and T. M. Rice, Science **271**, 618 (1996).
[4] R. Kumai, Y. Okimoto, and Y. Tokura, Science **284**, 1645 (1999).
[5] D. Trinschek and M. Jansen, Angew. Chem., Int. Ed. Engl. **38**, 133 (1999).
[6] T. Osafune *et al.*, Phys. Rev. Lett. **78**, 1980 (1997).
[7] E. Wigner, Phys. Rev. **46**, 1002 (1934).
[8] J. Hubbard, Phys. Rev. B **17**, 494 (1978).
[9] J. Solyom, Adv. Phys. **28**, 201 (1979).
[10] George Grüner, *Density Waves in Solids* (Addison-Wesley, Reading, MA, 1994).
[11] J. Voit, Rep. Prog. Phys. **58**, 977 (1995).
[12] K. Hestermann and R. Hoppe, Z. Anorg. Allg. Chem. **367**, 261 (1969).
[13] F. C. Zhang and T. M. Rice, Phys. Rev. B **37**, R3759 (1988).
[14] In the case of periodic boundary conditions $V_l = \max[V/l, V/(N - l)]$, where $1 < l < N$.
[15] Y. Mizuno *et al.*, Phys. Rev. B **57**, 5326 (1998).
[16] R. Weht and W. E. Pickett, Phys. Rev. Lett. **81**, 2502 (1998).
[17] For small hopping $S_c(q)$ is peaked at q_w irrespective of the signs of t_1 and t_2.
[18] D. C. Johnston *et al.*, Phys. Rev. B **61**, 9558 (2000).
[19] P. W. Anderson, Phys. Rev. **115**, 2 (1959).
[20] S. Tornow *et al.*, Phys. Rev. B **60**, 10206 (1999).
[21] J. Jaklič and P. Prelovšek, Adv. Phys. **49**, 1 (2000).
[22] S. R. White and I. Affleck, Phys. Rev. B **54**, 9862 (1996).
[23] M. Mayr *et al.* (to be published).